REVISTA INTERDISCIPLINAR DE PESQUISA EM ENGENHARIA

CILAMCE 2016
XXXVII IBERIAN LATIN AMERICAN CONGRESS ON COMPUTATIONAL METHODS IN ENGINEERING
BRASÍLIA - DF - BRAZIL

ANALYSIS OF THE RELATION BETWEEN THE FLEXURAL STRESS AND THE GEOMETRICAL VARIATIONS IN SPUR GEARS USING MODIFIED LEWIS' EQUATION AND NUMERICAL METHODS

Pedro M. S. Quadros

Victor T. Betim

Ana Paula C. S. Ferreira

Carlos Henrique da Silva

pedromsquadros@gmail.com

vbetim8@gmail.com

apaula@utfpr.edu.br

carloshs@utfpr.edu.br

Department of Mechanical Engineering, Technological Federal University of Paraná

Avenida Sete de Setembro, 3165, zip code 80230- 901,Curitiba, Paraná, Brazil

Abstract. *One of the failure types in spur gears is the teeth fracture caused by flexural stress in the tooth root region. In this way, this work objective is to validate and apply a numerical model to perform the flexural stress calculations in spur gears and evaluate the influence of some parameters in the stresses. Several works use numerical models validated by the stresses in the contact region calculated using the Hertz theory for nonuniform contact. However, when the interest is in the flexural stresses, it is considered more appropriate a validation based on the calculation of these stresses using solids mechanics concepts. In this paper the validation is done comparing the flexural stresses values calculated analytically and numerically in the critical point, which is in the tooth root. It is presented a modified Lewis' equation for the analytical calculation, which considers load in the HPSTC (Highest Point of Single Tooth Contact) and a stress concentration factor. Once a validated numerical model is gotten, the module, number of teeth, pressure angle, center distance and velocity ratio are varied. The flexural stresses of the gears are calculated for each geometrical variation aiming at to map the influence of each one of these parameters in reduction of the*

flexural stress. The results showed that the validation strategy adopted was effective. Furthermore, the gear module and the number of teeth are the parameters that most affect the flexural stress.

Keywords: *Stress concentration factor, Lewis' equation, Finite elements, Geometrical parameters, Flexural stress*

1 INTRODUCTION

The fracture due to flexural fatigue in gears happens while operating and in the most times occurs suddenly, causing significant damage. It is necessary that these machines elements, after projected and manufactured, do not work in conditions that let failure happen. For the improvement of gear projects it is important to know which geometrical parameters favor the reduction of flexural stresses. The parameters most commonly varied are module, number of teeth and pressure angle. Knowing the influence of each parameter in the stresses acting in the tooth root can represent significant profits in the project. In the last years the design of gears progressed in several lines, based on the development and better knowledge of the applied materials (Yamanaka et al, 2009; Burbank and Woydt, 2015), on the development and adaptation of devices for static and dynamic experiments (Xi, 2010; Li, Sosa and Olofsson, 2015) and in the use of numerical simulation, mainly with finite elements (Dayi et al, 2013; Pedrero et al, 2010).

The numerical simulation process is preceded by the development and validation of the numerical model. In this work the validation can be done by comparing the result of the numerical model with the analytical solution of Lewis or the solution presented by the AGMA 908-B89 (AGMA, 1989). Validating a numerical model is in general a rigorous process, because the compared models must be under the same conditions in order to get good results. Specifically in the present situation it becomes necessary a feasible path between the Lewis' equation that is quite simplified and the equation proposed by the AGMA norm, which includes several empirical or semi empirical coefficients difficult of being reproduced in the numerical model. In this way, it is proposed a modified Lewis' equation.

The traditional Lewis' equation, proposed by himself in 1892 and presented in several references (Norton, 2013; Mazzo, 2013), considers load in the tooth tip and does not include a stress concentration factor. In the analytical model of this work the modified Lewis' equation considers load in the HPSTC (Highest Point of Single Tooth Contact) and a stress concentration factor. The intensity of the flexural stresses in the teeth root of gears is directly related with the intensity and location of the applied load. In the HPSTC the loading applied causes the greater values of stress in the teeth root. The most critical loading only happens in the tooth tip when the contact ratio of the gears has unitary value. Since it is desired a model that considers several contact ratios, the most appropriate procedure is considering the load in the HPSTC as the most severe.

An important hypothesis that is adopted for the numerical simulation is related with de loading representation. Due to the fact that the tooth presents different stress values in its extension, while one tooth moves above another during the gearing, a dynamics analysis is the one that faithfully represents the phenomenon. However the numerical simulation in this work considers a static loading in the HPSTC. In this way the designing part responsible to evaluating the fatigue resistance of the tooth was not addressed, because the research goal is

to analyze the flexural stress in the tooth root for several geometrical configurations. The fatigue considerations can be included in a future work.

The region where the flexural stresses present the values of greater intensity is near tooth root. Therefore, it is necessary to know the geometrical characteristics that define the curvature of the tooth profile in its root. In this way, it is important, modeling the tooth profile of the gear according the manufacturing process. This gives reliable geometrical data for posterior use in analytical calculation and numerical simulation. The trochoid is traditionally used as the curve that connects the beginning of the involute with the radius of the root.

This work has as its objective evaluate the flexural stresses using numerical simulation, for that it is used a finite element commercial software. The important concepts used in the construction of the analytical model are presented in section 2. The construction and validation of the numerical model is presented in section 3. The results, presented in section 4, show the use of the numerical model in the calculation of flexural stresses at the critical point considering variations in the gear module, pressure angle, number of teeth, center distance and velocity ratio.

2 DEVELOPMENT

2.1 Modified Lewis' Equation

The Lewis' equation considers the tooth of the gear as a cantilever beam under transversal load. The beam base corresponds to the tooth root and the transversal load corresponds to the tooth tangential load. Therefore, this equation was developed based on one static analysis into a specific point of study located in the tooth root, called critical point. In Lewis' equation the flexural stress is calculated according Eq. (1).

$$\sigma = \frac{W_t}{F \cdot Y \cdot m}; \tag{1}$$

where W_t is the tangential force applied in the tooth, m is the gear module, F is the face width and Y is the geometrical factor or form factor of Lewis. This form factor considers the geometry of the tooth in order to determine its effective resistance in the root fillet. There is a table with the values of Y for gears of different pressure angles and number of teeth (Norton, 2013). However, in this work the form factor is calculated using Eq. (2), aiming at improving the compatibility between the numerical and analytical models.

$$Y = \frac{t^2}{6 \cdot l \cdot m}; \tag{2}$$

where t is the tooth thickness in the critical point and l is called height of the Lewis' parabole, both of them can be identified in Fig. 1. It presents the force components of a loading applied at the tooth tip and the critical point identification is given by letter A. In this point the flexural stresses are maximal and the shear stresses are null. The radial force component W_r is not considered, which means that the normal stresses of compression are disregarded in the formulation.

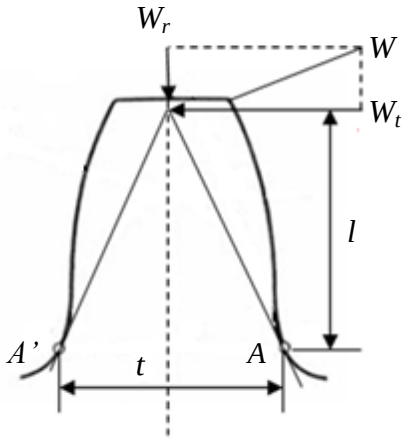

Figure 1 – Identification of the variables included in Lewis equation.

In a gearing with contact ratio between 1 and 2 the point where the load is not shared by more than one pair of teeth is the HPSTC. It means that, when the load is applied in this point, the tooth root is under the greater flexural stress. In this way, a first modification proposed related to the Lewis' equation is assume concentrated loading at HPSTC.

The stress concentration factor is another important parameter that is not considered in Lewis' analysis, but considered in this work. In this case, the maximum stress can be determined by Eq. (3).

$$\sigma_{\max} = \sigma_{nom} \cdot k_t; \tag{3}$$

where σ_{nom} is the stress gotten by Eq. (1) and k_t is the stress concentration factor. The calculation of k_t is detailed is section 2.4.

2.2 Loading conditions at HPSTC

The HPSTC can be visualized in Fig. 2, for its determination are used Eqs. (4) to (7) based on AGMA 908-B89 (1989). It is applied Eq. (4) to determine the transversal pressure angle, φ_r. The superior signal must be used when the gearing is external. After this calculation, one line that starts at the center of the gear with the angle of inclination ϕ_r and

length equal the base radius of the gear is created. C_6 is perpendicular to this line at R_{b2} length. The HPSTC is determined by the C_4 distance, defined at C_6 line.

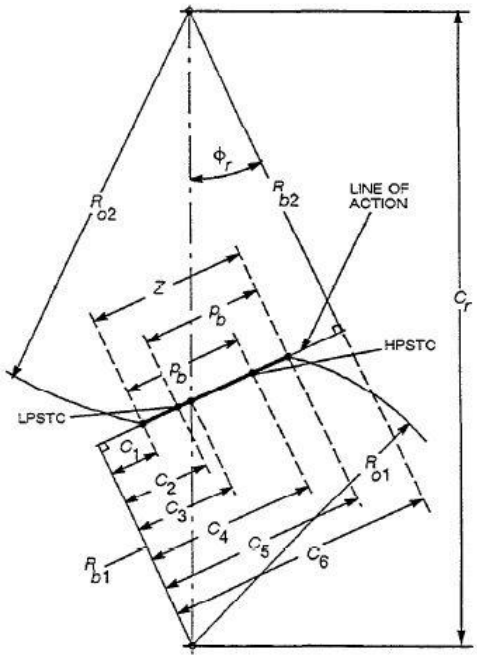

Figure 2 – HPSTC location (AGMA, 1989).

$$\phi_r = \cos^{-1}\left(\frac{R_{b2} \pm R_{b1}}{C_r}\right); \tag{4}$$

$$C_4 = C_1 + p_b; \tag{5}$$

$$C_1 = \pm\left[C_6 - (R_{o2}{}^2 - R_{b2}{}^2)^{0.5}\right]; \tag{6}$$

$$C_6 = C_r \cdot \sin\phi_r; \tag{7}$$

where:

- R_{b2} ; R_{b1} : base radius of gear and pinion
- C_r : center distance
- p_b : base pitch
- R_{o2} : gear external radius.

Having determined the HPSTC, it is possible to advance to the calculation of the load angle φ_{nL} and load radius r_{nL}, as in Eqs. (8) to (10) and in representation of Fig. 3.

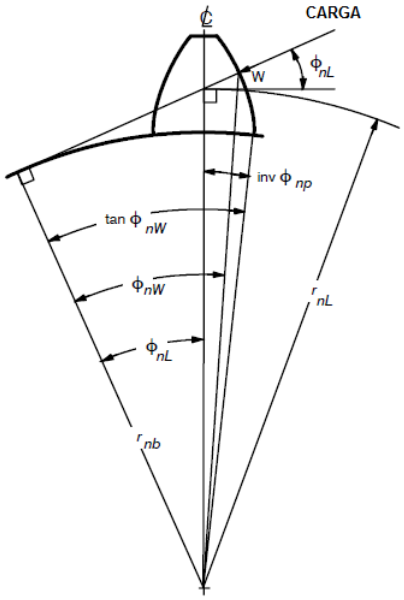

Figure 3 – Angle and radius of load (AGMA, 1989).

$$r_{nL} = \frac{R_{b1}}{\cos \phi_{nL}}; \tag{8}$$

$$\phi_{nL} = \tan \phi_{nW} - \tan \phi_r + \phi_r - \frac{S_n}{Z_1 \cdot m}; \tag{9}$$

$$\tan \phi_{nW} = \frac{C_4}{R_{b1}}; \tag{10}$$

where

- ϕ_r : pressure angle,
- S_n : tooth thickness in the pitch circle
- Z_1 : pinion teeth number
- ϕ_{nW} : pressure angle in the point of load application.

2.3 Critical point location

The method used for location of critical point is the one proposed by Broghamer and Dolan (1942). It is a four step procedure described below. Figure 4 helps in the understanding of the procedure.

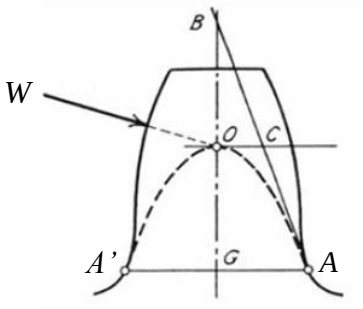

Figure 4 – Tooth profile for determination of the critical point by the geometrical method (Broghamer and Dolan, 1942).

- Draw the *OW* line in the load angle direction and normal to the tooth surface until intercept the center line *BG*;
- At point *O* draw the *OC* line perpendicular to the line *BG*;
- Draw the *AB* line with one of its tips tangent to the trochoid curve of the tooth root and the other coincident with the center line *BG*;
- Add the relation of equality on the length of the lines that compose *AB*, that is *BC* = *CA*. In this way *A* is the point of tangency between the tooth root curve and the Lewis' parabole. *AA'* is the line that joins the critical points of the two sides of the tooth.

The critical point location is necessary for getting the dimensions *t* (*AA'*) and *l* (*GO*), used in the calculation of the form factor presented in Eq. (2) and in the stress concentration factor presented in next section.

2.4 Calculation of the stress concentration factor

The calculation of the stress concentration factor uses Eq. (11) presented in the AGMA norm, this is the empirical relation developed by Broghamer e Dolan (1942) during their photoelastic experiments.

$$k_t = H + \left(\frac{t}{\rho_F}\right)^L \cdot \left(\frac{t}{l}\right)^M ; \tag{11}$$

where

$$H = 0.331 - 0.436 \cdot \phi_r ; \tag{12}$$

$$L = 0.324 - 0.492 \cdot \phi_r ; \tag{13}$$

$$M = 0.261 + 0.545 \cdot \phi_r ; \tag{14}$$

The variable ρ_F represents a minimum radius of curvature that the trochoid of the tooth root profile contains. According Pilkey (1997) the researcher Candee in 1941 developed the Eq. (15) that defines the relationship between the minimum radius of curvature ρ_F and the radius of the machining tool tip r_t.

$$\rho_F = \frac{(b - r_t^2)}{\frac{Z}{2 \cdot p_d} + (b - r_t)} + r_t ; \tag{15}$$

where b is the dedendum, p_d is the diametral pitch.

The concepts presented in the above sections make possible to construct an analytic solution more representative of real applications and a reliable numerical model. The use of the form factor of Lewis as presented in section 2.1 excludes the empirical information in the analytic stress calculation. Section 2.3 explains how to get the parameters used in the form factor computation. The inclusion of stress concentration factor in Lewis' equation, make the analytic solution more consistent with real applications. The calculation of the stress concentration factor is explained in section 2.4. Finally, applying the load in the HPSTC instead of in the tooth tip, make possible to use the analytic solution for gearings with aspect ratio greater than one. Section 2.2 explains how to get the load angle φ_{nL} and load radius r_{nL} corresponding to the HPSTC. These informations are used in the analytic and numerical model, in this way both use load application in same conditions.

3 METHODOLOGY

3.1 The involute and trochoidal profiles

The tooth profile of the majority of the external gears is composed of two curves: the involute and the trochoid. The intersection of these two curves occurs in the base diameter. Beneath the base diameter is the beginning of the trochoid, which ends in the root diameter. The trochoid is the curve of major interest for this study, since it defines the tooth root geometry. For the numerical model it is considered important assuring the involute and trochoid profiles for the tooth, since the analytical calculation is done in this premise. It was used the equations presented in Mazzo (2013) for the tracing of these curves in the model of this paper.

The trochoidal profile is related to the kind of manufacturing tool. For the teeth profiles of this work, it is considered that their generation will be done by a tool of the hob kind, without valley, because it is the most commonly used.

In both of the process of curves determination (involute and trochoid) a radius must be assigned in order to make possible a posterior calculation of the angle. These two parameters define the point position. This process is repeated by an amount of times equal to the number of point previously defined, for each assigned radius the set of equations is again applied. It is intuitive to notice that with the raising of the number of points, the curve profile becomes more precise.

3.2 Development and validation of the numerical model

The initial data for validation of the model are presented in Table 1. The parameters arbitrated are de teeth number of the pinion and gear, Z_1 and Z_2, respectively. Besides the pressure angle ϕ and the module m. RC is the contact ratio, which value is greater than one, justifying the consideration of load at the HPSTC. In this table also are presented the tangential force W_t, Poisson's ratio v and modulus of elasticity E.

Table 1 – Initial data for model development.

Z_1	Z_2	W_t (N)	ϕ (°)	m (mm)	RC	v	E (GPa)
21	35	760.9	20.0	5.0	1.63	0.29	205

The values used in the calculation of the load radius r_{nl} are presented in Table 2. The maximum flexural stress and values used in its calculation are presented in Table 3.

Table 2 – Load radius and other necessary parameters for its calculation.

r_{nL} (mm)	R_{b1} (mm)	ϕ_{nL} (°)	ϕ_{nW}(°)	S_n (mm)	C_4 (mm)
51.99	49.33	18.4	22.33	7.85	20.26
C_1 (mm)	p_b(mm)	C_6 (mm)	R_{o2} (mm)	R_{b2} (mm)	
5.51	14.76	47.88	92.5	82.22	

The teeth face width (F) is considered unitary in order to characterize plane stress. Furthermore, the radius of the tool tip (r_t) must be 30% of the module, according the catalogue of the hob kind tool. In this way, it was adopted r_t equal to 1.5 mm.

The trochoidal and involute profiles were done using the SolidWorks® software. The involute curve uses a linear distribution of points and the trochoid an exponential one, aiming at a greater precision of the tracing in the region near the tooth root.

Table 3 – Maximum flexural stress and necessary parameters for its calculation.

$\sigma_{máx}$ (MPa)	l (mm)	t (mm)	F (mm)	k_t	ρ_F (mm)	r_t (mm)
423.12	4.95	9.53	1	1.67	4.81	1.5

After finalizing the sketch, it was done the extrusion operation in order to create the pinion and its tooth. Since the simulation refers to loading into a single tooth, the inclusion of all ones just increases the computational cost of the analysis. The SolidWorks® model is then exported to the Abaqus® software.

In Abaqus the boundary conditions of the model are established and the loading is applied. Figure 5 shows the numerical model, its boundary conditions and applied load. As boundary conditions, the gear is fixed in relation to its center, for this the central point RP-1 is attached to the hole face of the pinion and configured with none degree of freedom. For the loading, it was applied the tangential component of the load (W_t), in its respective direction and distributed in the tooth width. RP-2 defines the location of the loading application.

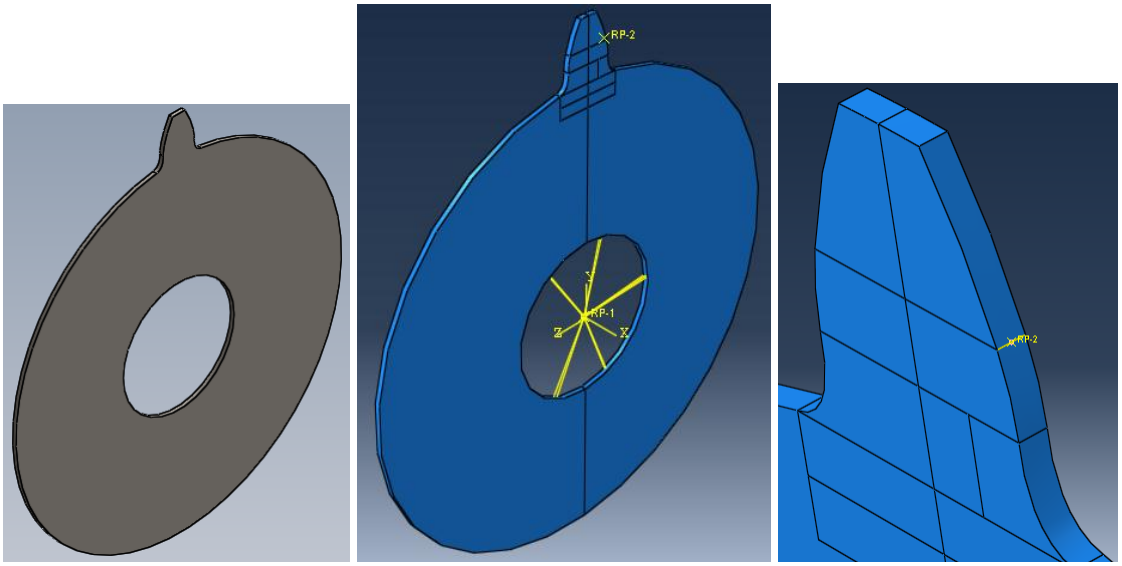

(a) (b) (c)

Figure 5 – Numerical model (a), boundary conditions definition (b) and loading application (c).

Hexagonal finite elements have been chosen for the simulation. Partitions were created in the model that makes possible refine the mesh in regions of interest. For the definition of the size of the elements in the mesh it was done a convergence analysis that is shown in Fig. 6. The size of the elements in this figure is related to the partition of the tooth root. The partitions and mesh configurations after the convergence analysis are presented in Fig. 7.

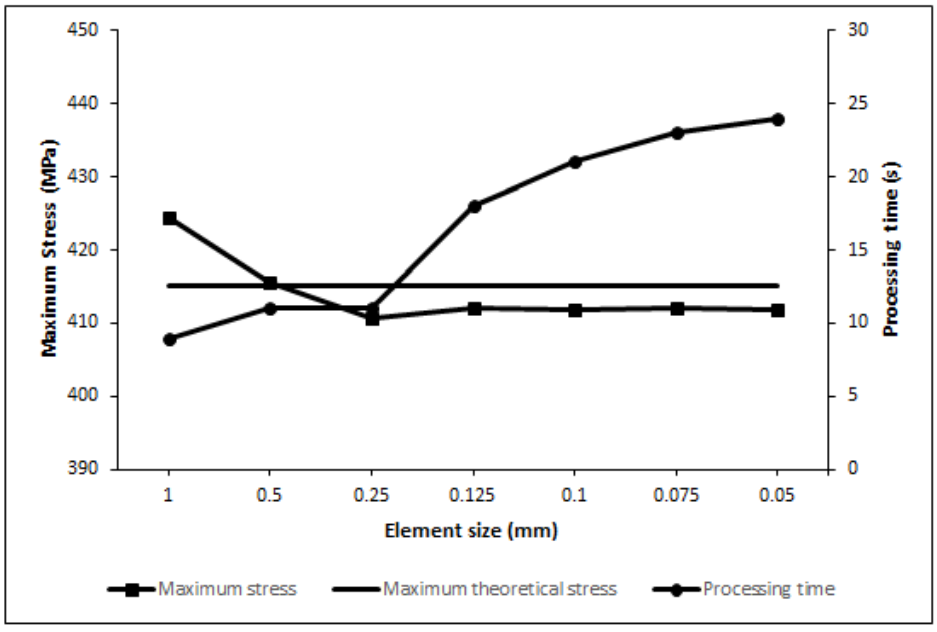

Figure 6 – Numerical model convergence analysis.

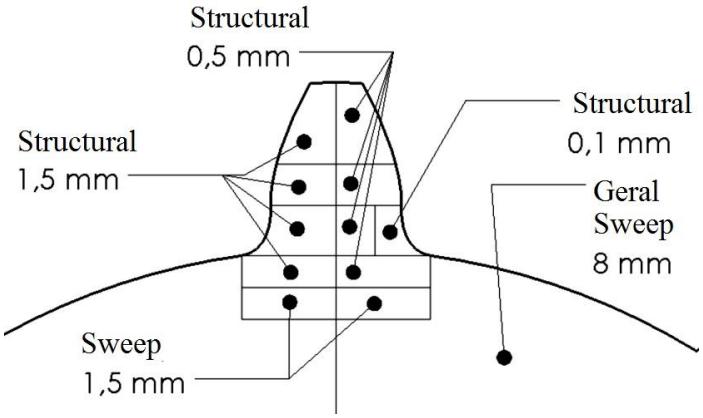

Figure 7 – Finite element mesh configuration.

It is possible to see that the stress obtained by numerical methods stabilizes in the element of size 0.125mm. Also, can be seen the increase of processing time when the mesh is refined. In this paper, it was used elements of size 0.1mm, so that guarantees an equilibrium between short processing time and good reliability. The maximum stress computed with this element size is 411.92 MPa. This corresponds to an error of 2.65% related to the analytical solution, and the numerical model is considered validated.

4 RESULTS

4.1 Flexural stresses for different configurations of pinion

The geometrical variations proposed for the configurations of the pinions are detailed in Table 4. For each group, three parameters are fixed and just one is varied, with the goal of making more evident the contribution of each one in the flexural stress. However, some parameters have dependent variations. For example, in analysis 1 to 8, changing Z implies in changing d_p. In analysis 9 to 16, changing m implies in changing Z. The velocity ratio is the only parameter that varies independently from the others.

In the numerical models used for getting results the applied force (W) is along the line of action with $\emptyset_{nL}$ contact angle. The tangential force (W_t) is used only in the validation of the numerical model, in order to compare with the analytical model that uses this tangential force. In this way, the results are presented in terms of Von Mises stresses, because this failure criterion includes the forces in the tangential and radial directions.

Table 4 – Configurations of the pinions for analysis of maximum flexural stress.

Analysis nº	Group	*i*	*m* (mm)	*Z*	d_p (mm)	σ' (Mpa)
1	m = 5 mm e ϕ = 20°	1:1	5	21	105	385.77
2				25	125	310.342
3				30	150	249.701
4				35	175	209.342
Analysis nº	**Group**	***i***	***m* (mm)**	***Z***	**d_p (mm)**	**σ' (Mpa)**
5	m = 5 mm e ϕ = 25°	1:1	5	21	105	337.538
6				25	125	272.599
7				30	150	221.093
8				35	175	187.144
9	dp = 120mm e ϕ = 20°	1:1	4	30	120	391.997
10			5	24	120	326.638
11			6	20	120	284.868
12			6.5	18	117	278.57
13	dp = 120mm e ϕ = 25°	1:1	4	30	120	346.596
14			5	24	120	286.622
15			6	20	120	248.977
16			6.5	18	117	243.017
17	dp = 100mm e ϕ = 20°	1:1	5	21	105	385.77
18		1:2		21	105	367.537
19		1:3		21	105	359.743
20		1:4		21	105	355.735
21	dp = 100mm e ϕ = 25°	1:1		21	105	337.538
22		1:2		21	105	322.443
23		1:3		21	105	316.249
24		1:4		21	105	312.892

Figure 8 presents the flexural stress distribution along the radius of the tooth root, for gears with number of teeth between 21 and 30. It is possible to notice that the flexural stress behavior can be approximated by polynomial functions. The coefficients of determination (R^2) are related to approximations with polynomial of third degree and they can be better if the degree of the polynomial is increased.

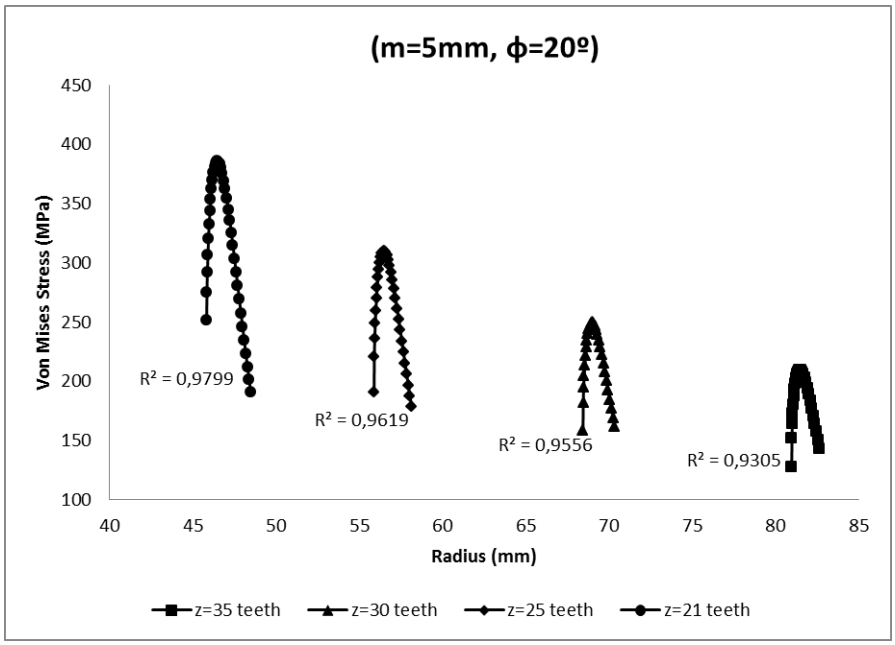

Figure 8 – Flexural stress distribution along the radius of gear tooth root.

Figure 9 presents the flexural stress behavior along the radius of the tooth root, now for gears with same configurations, except by the pressure angle. In these cases the flexural stresses can also be approximated by polynomials of third degree, with coefficients of determination near to one. Furthermore, the increase in the pressure angle reduces the tangential component of the force, which is more influent in the flexural stress. As expected, the flexural stress is smaller for larger pressure angles.

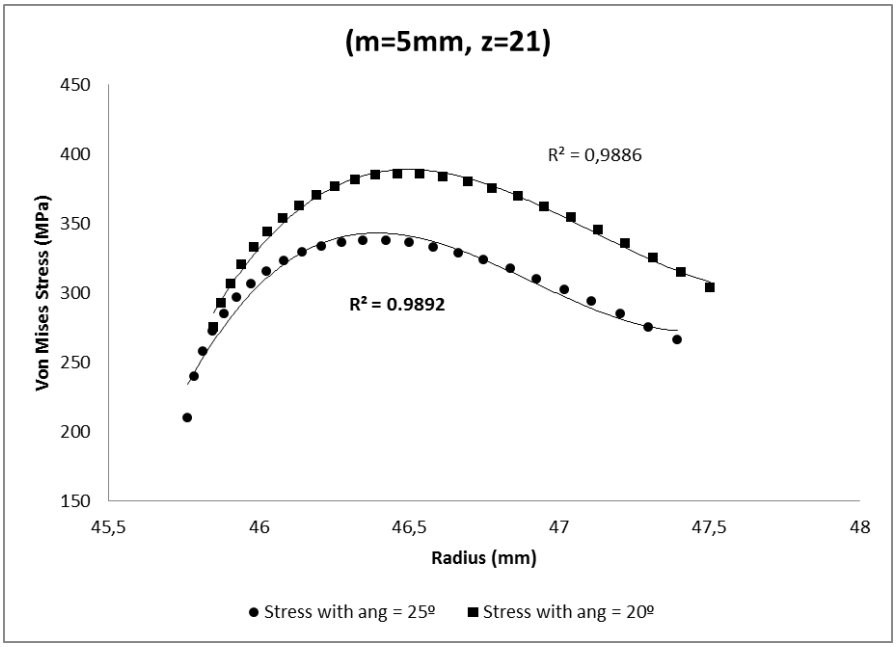

Figure 9 - Flexural stress distribution along the radius of gear tooth root, considering different pressure angles.

4.2 Flexural stress analysis for gears with different number of teeth

Figure 10 presents the stress values for different number of teeth in the pinion, and pressure angles of 20º and 25º. It is possible to notice that the stress is decreased with the increasing of the number of teeth. Furthermore, the flexural stress behavior can be approximated by polynomials of third degree with coefficient of determination equal to one.

It is also presented the increasing in the center distance corresponding to the increasing in the teeth number. This is an important information in the context of manufacturing, since is related to the size of the gear box. The intersection of the stress line with the center distance line corresponds to a balance point for the project.

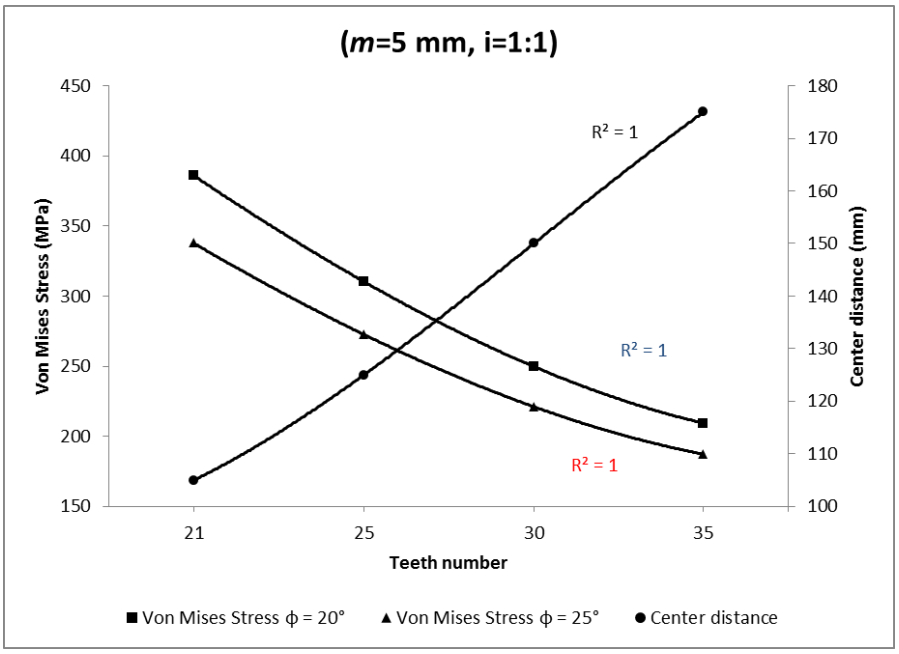

Figure 10 – Flexural stress and center distance versus teeth number.

Increasing the number of teeth from 21 to 35, the flexural stress is reduced in about 45% for both pressure angles. The stress decreasing with the number of teeth increasing is explained by the fact that these intensities are directly related with the geometrical characteristics of the tooth, as the height of the Lewis' parabola *l* and the tooth thickness in the critical point *t*. Analyzing Eqs. (1) and (2), it is possible to see that a reduction in *l* and an increasing in *t* results in flexural stress reduction.

The graphics of Fig. 11 show that with the increasing in the number of teeth, the height of Lewis' parabola is decreased and the tooth thickness in the critical point is increased. Consequently, the flexural stress is reduced. These data are for the same gears of Fig. 10. It is possible to notice that the height of the Lewis' parabola and the tooth thickness at the critical point are smaller for pressure angle equal to 20º. Smaller height of the Lewis' parabola, results in smaller flexural stress. However, a smaller tooth thickness at critical point, results in greater flexural stress. Since the thickness is a quadratic variable, it contributes more for the

increasing of the flexural stress. This also explains the fact that the flexural stresses are smaller for greater pressure angles.

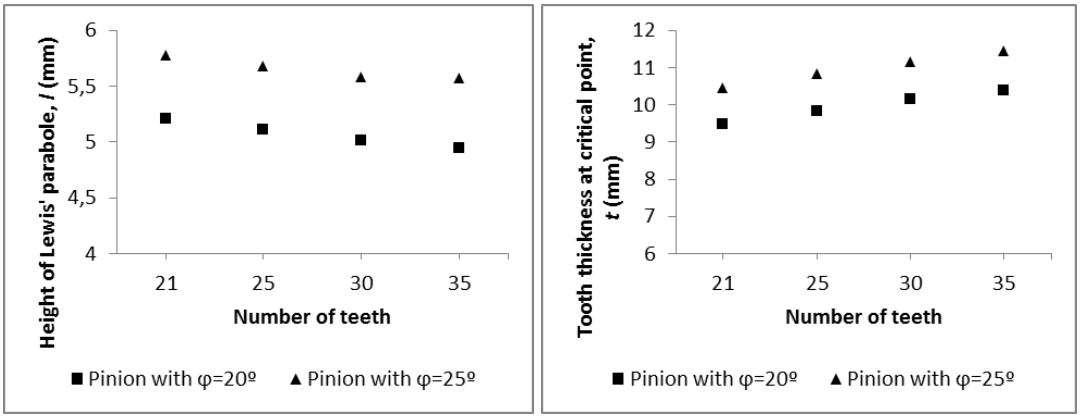

Figure 11 – Height of Lewis' parabole (*l*) and tooth thickness at critical point (*t*).

4.3 Flexural stress analysis for gears with different module

Figure 12 shows how the flexural stress varies when the module is changed. A module increasing causes a stress decreasing. Since the primitive diameter is constant, the number of teeth is reduced with the module increasing. The variation of the flexural stress and of the number of teeth can be approximated by polynomial of third degree, with coefficients of determination close to one.

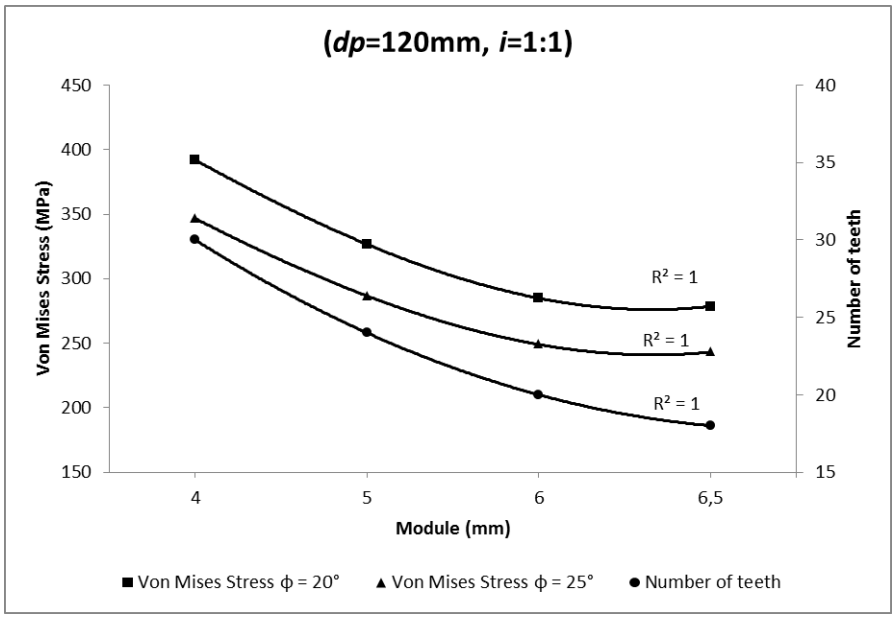

Figure 12 – Flexural stress and number of teeth versus module.

Increasing the module from 4mm to 6.5mm, the flexural stress is reduced in about 30% for both pressure angles. Equation (1) shows that stress is inversely proportional to the module, so this result is in agreement with the analytical solution.

4.4 Flexural stress analysis for different velocity ratio

Figure 13 show the values of flexural stress and HPSTC for different values of velocity ratio. The curves are approximated by polynomials of third degree with coefficient of determination equal to one. The continued lines represent Von Mises Stress and dashed lines represent the location of HPSTC in the *y*-coordenate.

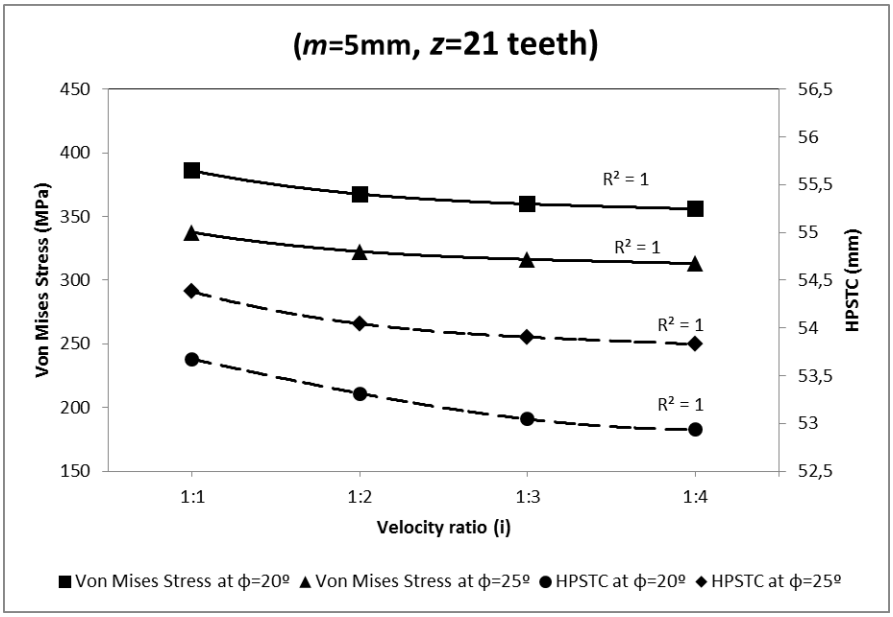

Figure 13 – Flexural stress and load radius versus velocity ratio (ϕ=25º).

Increasing the velocity ratio from 1:1 to 1:4, the flexural stress is reduced in 8%, for both pressure angles. It is possible to notice that the HPSTC point is smaller for bigger velocity ratio. An HPSTC point closer to the tooth root (consequently the load radius is also closer), results in smaller flexural stress. Furthermore, the flexural stress is smaller for pressure angle of 25º. This is explained by the fact that a bigger pressure angle has a smaller tangential force component and consequently a smaller flexural stress.

Figure 14 presents a summary of the 24 analysis performed. Analysis 8 is the best configuration for reducing the flexural stress. According Table 4 in this analysis the pressure angle is 25 degrees, the module is 5 mm, the velocity ratio is 1:1 and number of teeth is 35. A case that indeed has values parameters that favor the reduction of flexural stress as bigger pressure angle and number of teeth and intermediary module. It is in agreement with the observations of the previous subsections.

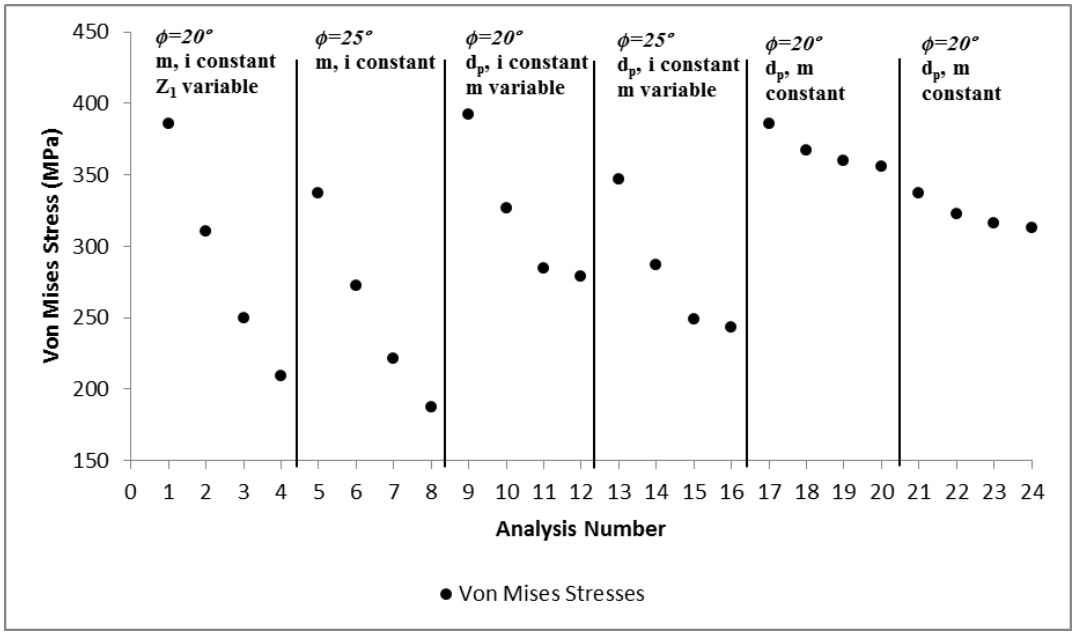

Figure 14 – Flexural stress for all analysis performed.

Looking at Figure 14 it is possible to conclude that a pinion with 30 teeth and pressure angle of 25° (analysis 7) has almost the same flexural stress that a pinion with 35 teeth and pressure angle of 20° (analysis 4). In the same way, a design with velocity ratio of 1:1 and pressure angle of 25° (analysis 21) has almost the same result in terms of flexural stress that a design with velocity ratio of 1:4 and pressure angle of 20° (analysis 20). The alternatives of design become clearer when all the analysis performed are put together.

5 CONCLUSIONS

The present work proposes the validation of a numerical model for calculating flexural stress in tooth root of gears using Lewis' equation. The Lewis's equation considers load in the tooth tip and does not considers stress concentration factor. Therefore, it is presented a modified Lewis' equation, which considers load in the HPSTC and includes a stress concentration factor. It was gotten good agreement between the numerical and analytical models with this approach.

Having a validated numerical model, were defined three main groups of results. In group one (analysis 1 to 8) the module, pressure angle and velocity ratio are constant and the number of teeth and, consequently, center distance are variable. In group two (analysis 9 to 16) the center distante, pressure angle and velocity are constant and the module and, consenquently, number of teeth are variable. In group three (analysis 17 to 24) the center distance, pressure angle, module and number of teeth are constant and the velocity ratio is variable.

The results showed that increasing the number of teeth from 21 to 25, the flexural stress is reduced in about 45% for both pressure angles. Furthermore, increasing the module from 4 mm to 6.5mm, the flexural stress is reduced in 30% for both pressure angles.

In analysis where it was varied the velocity ratio, the flexural stress reduction is less accentuated. Increasing the velocity ratio from 1:1 to 1:4, the flexural stress is reduced in 8%. Anyway, since velocity ratio is in general the primary goal of the transmission, it is not usual a design with flexibility in this requirement. The flexural stress for pressure angle of 25º is in average 15% smaller compared to the flexural stress for pressure angle of 20º, for analysis in same conditions.

The results make possible to conclude that the flexural stress is more sensitive to changes in module and number of teeth, having it value significantly altered when these parameters are changed.

ACKNOWLEDGEMENTS

The authors want to thank to Technological Federal University of Paraná.

REFERENCES

AGMA, 1989. American Gear Manufactures Association, AGMA 908 - B89: geometry factors for determining the pitting resistance and bending strength of spur, helical and herringbone gear teeth. Alexandria.

Broghamer, E. L. and Dolan, T. J., 1942. A photoelastic study of stresses in gear tooth fillets. Engineering experiment station. Illinois, vol. 39, pp. 24-39.

Burbank, J. and Woydt, M., 2015. Comparison of slip-rolling behavior between 20MnCr5 gear steel, 36NiCrMoV1-5-7 hot working tool steel and 45SiCrMo6 spring steel. Wear, vol. 328-329, pp. 28-38.

Dayi, Z., Shuguo, L., Baolong, L. and Jie, H., 2013. Investigation on bending fatigue failure of a micro-gear through finite element analysis. Enginering Failure Analysis, vol. 31, pp. 225-235.

Li, X., Sosa, M. and Olofsson, U., 2015. A pin-on-disc study of the tribology characteristics of sintered versus standard steel gear materials. Wear, vol. 340-341, pp. 31-41.

Mazzo, N., 2013. Engrenagens cilíndricas: Da concepção à fabricação. 1. ed. São Paulo: Blucher.

Norton, R. L., 2013. Projeto de Máquinas: Uma abordagem integrada. 4. ed. Porto Alegre: Bookman.

Pedrero, J. I., Pleguezuelos, M., Artés, M. and Antona, J. A., 2010. Load distribution model along the line of contact for involute external gears. Mechanism and Machine Theory, vol. 45, pp. 780-794.

Pilkey, W. D.,1997. Peterson's stress concentration factors. 2. ed. New York: John Wiley & Sons, Inc.

Xi, L., 2010. Investigation of the region of fatigue crack initiation in a transmission gear. Materials Science and Engineering A. vol. 527, pp. 1377-1382.

Yamanaka, M., Tamura, R., Inoue, K., Narita, Y. Y., 2009. Bending fatigue strength of austempered ductile iron spur gears, Journal of advanced mechanical design, systems, and manufacturing. vol. 3, n. 3, pp. 203-211.